

A Damped Oscillator Model for Infrared Spectra of Formamide in the Liquid State

Isao Kanesaka[*,†] **and Eiji Mitsuhashi**

Faculty of Science, Toyama University, 3190 Gofuku, Toyama 930-8555

Received August 29, 2007; E-mail: kanesaka@po6.nsk.ne.jp

Infrared spectra of formamide are wholly simulated for the in-plane modes on the basis of a damped oscillator model, where force constants and intensity parameters and damping constants defined in every Cartesian displacement coordinate are simultaneously adjusted. Band constants evaluated from the damped oscillator model are compared with those observed. The present analysis reveals the relation in band widths among all vibrational modes, in other words, the origin of band widths. Large values of the damping constant on H in the NH_2 group result from inter-molecular interactions, i.e., hydrogen bonds. Unexpected results of the damping constants on O, C, and N are discussed with van der Waals forces and intra-molecular interactions.

It is well-known that the band profile of a vibrational mode is given by the damped oscillator model, where the equation of motion with a frictional force is treated under an oscillating external force. This model was developed to a two-mode system by Barker and Hopfield[1] and to a many-body system by Chaves et al.[2] We have applied the two-mode system to the analyses of dips in infrared spectra of ammonium dihydrogen phosphate,[3] the band profile of C≡N stretching bands of binary KOCN-KSCN aqueous systems[4,5] and the band profile of C=O stretching bands of acetone.[6] In these analyses mechanical and damping coupling constants are used, resulting in spectral features similar to NMR due to the Bloch equation with chemical exchanges.

Although the above damped oscillator model describes the band profile of a system consisting of normal modes, it may be possible to develop it for the analysis of the whole band profile of vibrational spectra of a polyatomic molecule. This may be possible by constructing the equation of motion on the basis of the GF matrix method, treating simultaneously oscillating external forces and frictional forces, as done for the damped oscillator model described above. This damped oscillator model will be described in detail as well as the analytical procedures.

In the present analysis, we neglect a transition-dipole coupling between adjacent molecules, which results in the splitting of a strong infrared band, as reported for C=O stretching bands of acetone.[6] Hydrogen bonds and/or molecular associations are also neglected. That is, the observed infrared spectrum is analyzed on the basis of a single molecule. The analysis was carried out for the in-plane modes of formamide, which is a viscous liquid with a high dielectric constant,[7] suggesting the importance of motion accompanying a frictional force.

Many authors[8–24] have investigated infrared and Raman spectra of formamide in the gaseous, liquid and solid states. Normal coordinate analysis has been done for the in-plane modes of formamide[10,15] and for the whole modes including lattice ones.[12] In the liquid state, hydrogen-bonded chain structures are suggested from Raman studies of mixtures of isotopomers[18–21] and low-wavenumber vibrational spectra,[16,17,22] although cyclic dimers[15] and trimers[9] of formamide are proposed. The solution spectra[8,9,14,15,23,24] were studied in relation to liquid structures and binary adducts.

Damped Oscillator Model

The equation of motion of a polyatomic molecule interacting with radiation field $\mathbf{E}(\nu)$ may be given as[1,25]

$$\mathbf{M}\ddot{\mathbf{X}} + \tilde{\mathbf{B}}\,\mathbf{FBX} = \mathbf{eE}(\nu), \tag{1}$$

where $\mathbf{M}$ and $\mathbf{F}$ are the mass and force constant matrixes, respectively, and $\mathbf{B}$ is defined as $\mathbf{R} = \mathbf{BX}$, where $\mathbf{R}$ and $\mathbf{X}$ are the internal and Cartesian displacement coordinate matrixes, respectively, and $\mathbf{e}$ is the intensity parameter column matrix with element e. By use of the frictional force matrix or the damping constant matrix, $\boldsymbol{\gamma}$, which is a square diagonal matrix with element γ, Equation 1 is re-written as

$$\mathbf{M}(\ddot{\mathbf{X}} - \boldsymbol{\gamma}\dot{\mathbf{X}}) + \tilde{\mathbf{B}}\,\mathbf{FBX} = \mathbf{eE}(\nu). \tag{2}$$

On the basis of the forced vibration, Equation 2 is re-written as

$$(-\nu^2\mathbf{U} - \mathrm{i}\nu\boldsymbol{\gamma})\mathbf{X}_\mathrm{M} + \mathbf{M}^{-1/2}\tilde{\mathbf{B}}\,\mathbf{FBM}^{-1/2}\mathbf{X}_\mathrm{M} = \mathbf{tE}_\mathrm{o}, \tag{3}$$

where $\mathbf{U}$ is the unit matrix, $\mathbf{E}_\mathrm{o}$ the amplitude of $\mathbf{E}(\nu)$, $\mathbf{X}_\mathrm{M} = \mathbf{M}^{1/2}\mathbf{X}$ and $\mathbf{t} = \mathbf{M}^{-1/2}\mathbf{e}$; $\mathbf{t}$ is the column matrix with element t. By defining $\mathbf{G}^{-1}(\nu)$ as

$$\mathbf{G}^{-1}(\nu) = (-\nu^2\mathbf{U} - \mathrm{i}\nu\boldsymbol{\gamma}) + \mathbf{M}^{-1/2}\tilde{\mathbf{B}}\,\mathbf{FBM}^{-1/2}, \tag{4}$$

we have

$$\mathbf{X}_\mathrm{M} = \mathbf{G}(\nu)\mathbf{tE}_\mathrm{o} = \mathbf{G}(\nu)\mathbf{t}, \tag{5}$$

in $\mathbf{E}_\mathrm{o} = \mathbf{1}$. The linear response function or the infrared spectrum is given as

$$S(\nu) = \nu\,\mathrm{Im}\,\tilde{\mathbf{e}}\mathbf{X} = \nu\,\mathrm{Im}\,\tilde{\mathbf{e}}\mathbf{M}^{-1/2}\mathbf{X}_\mathrm{M} = \nu\,\mathrm{Im}\,\tilde{\mathbf{t}}\mathbf{G}(\nu)\mathbf{t}, \tag{6}$$

where Im means the imaginary part.

$S(\nu)$ is drawn by use of the initial sets of $\mathbf{F}$, γ, and $\mathbf{t}$, by

† Present address: Meirin-cho 1-242 717, Toyama 930-0001

Published on the web February 12, 2008; doi:10.1246/bcsj.81.248

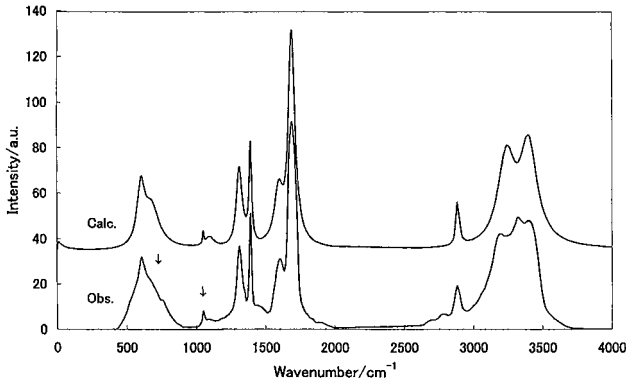

Fig. 1. The observed and calculated infrared spectra of formamide in the liquid state. The band arrowed are the out-of-plane modes.

changing ν, and they are simultaneously adjusted by the least-squares method.

Results and Discussion

Figure 1 shows the observed infrared spectrum of formamide in the liquid state, where the bands arrowed are the out-of-plane modes. In the region of the NH_2 stretchings there are three strong bands at 3404, 3329, and 3190 cm^{-1} with a weak band at 3248 cm^{-1}. The highest band has been assigned to the NH_2 asymmetric stretching and the lower two to the Fermi doublet due to NH_2 symmetric stretching and the overtone of NH_2 bending,[14] although the four bands are due to a distorted cyclic dimer.[15] In the present analysis, the NH_2 symmetric stretching is assumed to be 3257 cm^{-1} in the intermediate between two bands at 3329 and 3190 cm^{-1} by inference from two N–D stretching bands observed in the infrared and Raman spectra of $HCOND_2$.[14] The C=O stretching is observed at 1690 cm^{-1} with a shoulder at 1712 cm^{-1}. The former and the latter are assigned to C=O stretchings due to hydrogen-bonded molecules and monomers or molecules at the end of a chain, respectively,[9,18] although an asymmetric infrared band profile is calculated on the basis of a transition-dipole coupling mechanism and liquid structures derived from molecular dynamics simulations.[22] In the isotropic Raman spectrum the C=O stretching is observed at 1668 cm^{-1},[18] which is weak in the infrared spectrum. In the present analysis, only the main band at 1690 cm^{-1} is used, although a large discrepancy in the region of the shoulder at 1712 cm^{-1} between the observed and calculated spectra is inevitable.

In the present analysis, formamide is assumed to be planar.[26–28] Figure 2 abbreviates the atom index, s, for each atom as A^s; s is used to note t or γ of the s atom as t^s or γ^s, respectively. The bond lengths, r, and the angles used are: r(C=O) = 1.22, r(C–N) = 1.35, r(C–H^3) = 1.10, and r(N–$H^{5,6}$) = 1.00 in Å, and ∠OCH^3 = 120.9, ∠OCN = 124.5, ∠CNH^5 = 118.4, and ∠CNH^6 = 119.6 in degrees.[28] The stretching and bending internal coordinates are denoted as Δr(A–B) and δ(ABC), respectively. The stretching force constant, K, the bending force constant, H, and the non-bonding force constant, F, are initially transferred from those reported by Suzuki[10] and somewhat modified. The band profile, especially the band width, depends considerably on force constants. Hence, many interaction force constants, I_i, were examined to obtain the coincidence between

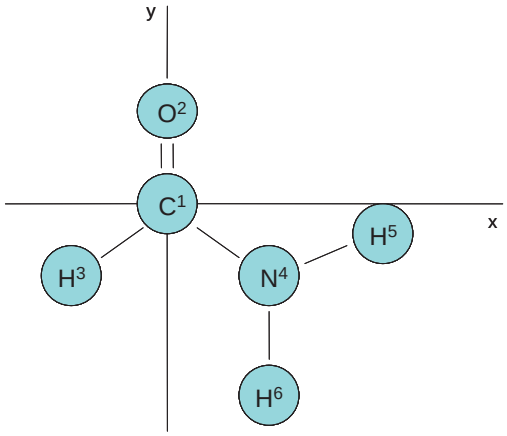

Fig. 2. The abbreviation of the atom index in formamide.

Table 1. The Force Constants[a] of Formamide in the Damped Oscillator Model

K(C–H^3)	359.2	H(OCH^3)	40.1
K(C=O)	801.6	H(OCN)	68.6
K(C–N)	711.1	H(H^3CN)	41.7
K(N–H^5)	571.8	H($CNH^{5,6}$)	49.5
K(N–H^6)	613.4	H(H^5NH^6)	42.2
F(C···H^5)	23.4		
F(C···H^6)	26.7		
F(O···H^3)	86.4		
F(O···N)	135.4		
F(H^3···N)	65.4		
I_1(C=O, C–N)	−11.8		
I_2(C=O, NH_2)	−4.5		
I_3(C=O, H^3CN)	4.7		
I_4(C–N, H^3CN)	13.6		
I_5(C–N, CNH^6)	27.4		

a) K, F, I_1 in N m^{-1}, I_2–I_5 in 10^{-10} N rad^{-1}, and H in 10^{-20} N m rad^{-2}.

the observed and calculated spectra, especially in the regions of the C=O stretching, NH_2 bending, C–H bending, and C–N stretching; hereafter, the vibrational mode is abbreviated by ν_i, as given in Table 2. I_1, I_2, and I_5 in Table 1 are effective on the band widths of ν_4 and ν_7, and I_3 and I_4 on that of ν_6. As a result, 20 force constants were used and are probably reliable. They are given in Table 1. We examined another set of force constants to reduce the number of constants. For example, the initial set of constants was transferred from those reported by Gardiner et al.,[15] who used only nine. However, a good fit was not obtained, even though additional interaction force constants (at least 5) were used because of large coupling between Δr(C=O) and $\delta(NH_2)$ or $\delta(H^3CO)$, which resulted in strong intensities of ν_5 and ν_6 and a large band width of ν_6; the sharp band width of ν_6, 20 cm^{-1}, is one of the spectral features in the present system. In the numerical fittings, the two out-of-plane modes, C–H out-of-plane bending at 1050 cm^{-1} and NH_2 wagging at 685 cm^{-1}, were simultaneously adjusted by use of a Lorentzian-like band (See Eq. 8) and some combination bands observed, for example, at 2850 and 1460 cm^{-1} were treated by lowering the weights.

Intensity parameters may originate from atomic charges.

Table 2. The Peak Positions, the Damping Constants and the Intensity Parameters of Formamide in the Damped Oscillator Model

	Peak position $\tilde{\nu}_i$/cm^{-1}		
Mode	Obs.	Calc. 1	Assignment
ν_1	3404	3399	NH_2 asym. str.
ν_2	3324, 3190	3239	NH_2 sym. str.
ν_3	2882	2887	C–H str.
ν_4	1690	1690	C=O str.
ν_5	1608	1597	NH_2 bend.
ν_6	1391	1392	C–H bend.
ν_7	1309	1310	C–N str.
ν_8	1090	1094	NH_2 rock.
ν_9	608	602	OCN bend.

	Damping constant γ^s/cm^{-1}		Intensity parameter[a] t^s or e^s/au			
Atom	γ^s_x	γ^s_y	t^s_x	e^s_x	t^s_y	e^s_y
C^1	46	64	10.7	37.1	23.0	80.5
O^2	70	27	−10.3	−41.2	−20.0	−80.0
H^3	38	4	14.5	14.5	2.2	2.2
N^4	34	43	−13.1	−48.9	−12.1	−45.2
H^5	190	76	35.0	35.1	16.3	16.4
H^6	79	160	4.2	4.2	26.9	26.9
		$\sum e^s$		0.9		0.8

a) t^s and e^s are related as $\mathbf{t} = \mathbf{M}^{-1/2}\mathbf{e}$ (See Eq. 3).

Hence, those of O and N were initially taken to be negative and those of the others positive. On the other hand, the x and y components of t^s differ. Since such a difference results from the fact that, for example, the intensity of the N–H stretching is stronger than that of the N–H bending or rocking, giving rise to the larger value of t parallel to the N–H bond than that perpendicular to the N–H bond, the two components may be independent. The intensity of the translational mode to the x direction is given as

$$S_T = \left(\sum e^s \Delta x_s\right)^2 = \left(\sum e^s\right)^2 \Delta {x_o}^2, \tag{7}$$

by inferring that the displacements of all atoms are the same. Since S_T should be zero, the relation of $\sum_s e^s = 0$ may hold for both the x and y directions. In the numerical fitting, the intensity parameters were adjusted for $S(\nu)$ in Eq. 6 to be zero at $\nu \approx 0$, which almost satisfies the condition of Eq. 7, as shown later (Table 2), although $S(\nu)$ at $\nu \approx 0$ has non-zero values due to the intensity of a rotational mode. Since the intensity parameters are defined relatively, the results of deducing one unknown parameter may be reliable.

Three of 12 damping constants were assumed in the course of numerical fitting as follows: The largest value was 190 cm^{-1} for γ^5_x by inference from the band width of NH_2 stretching. The smallest assumed value was γ^3_y, 4.0 cm^{-1}, from the sharpness of ν_6. The relation of $\gamma^6_x \approx \gamma^5_y$ was also assumed. The assumed value of γ^s and the reliability of γ^s are also discussed later and in the Appendix. The others were adjusted in the usual way. The calculated wavenumber of the i-th mode, $\tilde{\nu}_i$, obtained from $\mathbf{M}^{-1/2}\tilde{\mathbf{B}}\,\mathbf{FBM}^{-1/2}$, and the values of t^s and γ^s are summarized in Table 2, where the components of $\mathbf{e}$ ($= \mathbf{M}^{1/2}\mathbf{t}$) are also given. The calculated spectrum is given in Fig. 1.

In Fig. 1, the calculated spectrum coincides closely with the observed one, except for the regions of ν_1, ν_2, and ν_4. As expected from the formulation of the damped oscillator model, the band profile of the i-th mode is approximately given as

$$S_i(\nu) \approx \nu \,\mathrm{Im}\, \frac{T_i^2}{\tilde{\nu}_i^2 - \nu^2 - i\nu\Gamma_i}, \tag{8}$$

where T_i and Γ_i are the effective intensity parameter and the damping constant, respectively. That is, the band profile is approximately given by the Lorentzian. T_i and Γ_i may be evaluated from $\mathbf{t}$ and $\boldsymbol{\gamma}$ using the eigen vector, $\mathbf{L}$, of $\mathbf{M}^{-1/2}\tilde{\mathbf{B}}\,\mathbf{FBM}^{-1/2}$, as

$$\mathbf{T^c} = \tilde{\mathbf{L}}\mathbf{t} \tag{9}$$

and

$$\mathbf{\Gamma^c} = \tilde{\mathbf{L}}\boldsymbol{\gamma}\mathbf{L}, \tag{10}$$

respectively. The numerical results of Eqs. 9 and 10 are given in Calc. 1 in Table 3; since T_i due to Eq. 9 consists of the x and y components, $T_{ix} = \sum_s t^s_x l_{si}$ and $T_{iy} = \sum_s t^s_y l_{si}$, respectively, the total intensity, $S_i = (T_{ix})^2 + (T_{iy})^2$, is given in Table 3; l_{si} is the matrix element of $\mathbf{L}$ on the i-th mode. Γ_i consists of the contribution of γ^s as $\Gamma_i = \sum_s \gamma^s l^2_{si}$. In Table 3 the damping constant distribution, d.c.d., defined as $100\gamma^s l^2_{si}/\Gamma_i$, which corresponds to the potential energy distribution in normal coordinate analysis, is given for large values as, for example, $35\gamma^1_x$, which means that 35% of Γ_i is due to the term γ^1_x.

To confirm that the observed spectrum is described approximately in terms of $S_i(\nu)$ in Eq. 8 with band constants S_i and Γ_i, the observed spectrum was decomposed in the usual way using Eq. 8 with the equality sign for each band (model

Table 3. Band Constants of Formamide by the Damped Oscillator Model (Calc. 1) and the Model without Coupling (Calc. 2)

	Peak position/cm^{-1}	Intensity S_i/au		Band width Γ_i/cm^{-1}		
Mode	Obs.	Calc. 2	Calc. 1	Calc. 2	Calc. 1	d.c.d.
ν_1	3404	1024	1013	153	148	$88\gamma_y^6$
ν_2	3257	945	917	153	149	$75\gamma_x^5 + 13\gamma_y^5$
ν_3	2882	104	89	38	29	$85\gamma_x^3$
ν_4	1690	729	833	53	56	$52\gamma_y^1 + 10\gamma_y^5$
ν_5	1608	287	295	72	76	$41\gamma_x^6 + 26\gamma_y^5 + 17\gamma_x^5$
ν_6	1391	145	138	20	22	$41\gamma_x^3 + 13\gamma_y^2 + 11\gamma_y^3$
ν_7	1309	291	276	54	52	$35\gamma_x^1 + 22\gamma_x^5 + 15\gamma_x^4$
ν_8	1090	56	62	91	81	$38\gamma_x^6 + 32\gamma_x^5 + 14\gamma_y^5$
ν_9	608	285	264	71	64	$29\gamma_x^2 + 14\gamma_y^5 + 12\gamma_x^1$

without coupling). The decomposition was carried out by use of 11 bands of 9 in-plane modes and 2 out-of-plane modes. The band constants by a model without coupling are given in Calc. 2 in Table 3.

In Table 3 the differences in S_i and Γ_i between Calcs. 1 and 2 are within $\pm 14\%$, except for Γ_3, which is -24%. This confirms that Eqs. 9 and 10 give approximately the band intensity and width, respectively. It should be noted that the real band intensity and width in Calc. 1 are somewhat different with S_i and Γ_i, because $\mathbf{\Gamma^c}$ in Eq. 10 is not diagonalized, having considerable values, -26–$22\,\mathrm{cm}^{-1}$, in the off-diagonal elements. This is also true for the band profile, which is somewhat different with the additive one of component bands[4,5] (See also Appendix). Since the observed band profile is, of course, not the additive one of component bands, the values of γ^s are adjusted so as to make their reliability higher. In the other words, the observations about the band widths are more than the number of the in-plane modes, suggesting the adequacy of assumptions for γ^s described above. It should be also noted that the values of the off-diagonal elements in $\mathbf{\Gamma^c}$ indicate the possibility of a damping coupling with a plus or minus sign between fundamentals in the liquid state.

The strong intensities of ν_1 and ν_2 in Table 3 result in the large values of t_x^5 and t_y^6 in Table 2. The intensity of ν_4 is mainly attributed to the term t_y^1 and partly to the term t_y^2 because $|l_{74}| \approx 2l_{84}$; when s in l_{si} is larger than 6, s specifies the atom s-6 and l_{si} indicates the element on the y direction. The intensity of ν_5, 295, is quite larger than that of ν_8, 62, which results from the difference in the coupling with Δr(C–N). The effective intensity of ν_7 is not attributed to terms t_x^1 and t_x^4, that is Δr(C–N), because they cancel with term t_x^5, but to terms t_y^1 and t_y^2, that is Δr(C=O). The relation of $e_x^s \approx e_y^s$ is only obtained in N and the large differences in the other atoms reflect that the intensity of the stretching is larger than that of the bending, as noted above. In the present analysis $\sum_s e^s = 0$ in Eq. 7 is almost satisfied for both the x and y components, as seen in Table 2.

The fact that the band width is approximately given by $\Gamma_i = \sum_s \gamma^s l_{si}^2$ means that the band widths of ν_1–ν_9 are not independent but relate closely with each other, as normal frequencies relate to force constants. As seen in Table 3, the band width of ν_4 is mainly attributed to the term γ_y^1 (52%) and only partly to γ_y^2 (7%). This is a result unexpected from the hydrogen bond of O with H^5 or H^6, which suggests a large contribution of γ_y^2 to Γ_4, because a damping constant, that is a friction constant, relates to the second derivative of a potential function, $u(r)$, between the atom noted and adjacent molecules or atoms with respect to the molecular or atomic distance, i.e., the effective force constant; γ is given as[29,30]

$$\gamma = \frac{\rho_m}{36\pi m^2 c^3}\left[\int \nabla^2 u(r) g(r) \mathrm{d}^3 r\right]^2, \tag{11}$$

where ρ_m is the mass density of the fluid, m the mass of the particle, c the velocity of sound, and $g(r)$ a pair correlation function. The fact that the value of γ_y^2, $27\,\mathrm{cm}^{-1}$, is quite smaller than that of γ_y^1, $64\,\mathrm{cm}^{-1}$, is also unexpected from the hydrogen bond. Since C interacts with adjacent molecules or atoms by van der Waals forces, the large value of γ_y^1 indicates that the effective force constant due to van der Waals forces is larger than that due to hydrogen bonding (the component parallel to the C=O bond); it should be noted that the value of γ_x^2, $70\,\mathrm{cm}^{-1}$, may be consistent with the hydrogen bond. The van der Waals radius of C is largest in the atoms of formamide and the surface area too, resulting probably in the large effective force constant. The value of γ_y^2 is also smaller than those of N, γ_x^4 and γ_y^4, as seen in Table 2. This suggests frictional forces due to not only inter-molecular interaction but also intra-molecular interactions. C and N form covalent bond with three adjacent atoms, whereas O forms only with C. Hence, the formers may be more acted on by larger intra-molecular frictional forces than the latter, resulting in larger values of γ^1 and γ^4 than that of γ_y^2.

The band width of ν_6 is attributed mainly to the term γ_x^3 (41%), and is quite sensitive to γ_y^3 (11%), giving rise to the assumed value of γ_y^3 ($4\,\mathrm{cm}^{-1}$). The band widths of ν_5 and ν_8 are 76 and 81 cm^{-1}, respectively, and their close values are realized from d.c.d. in Table 3, where the magnitude of each term corresponds well to each other. In Table 2 the values of γ_x^5 and γ_y^6 are quite larger than that of γ_x^3. This indicates clearly that the damping constant relates to the hydrogen bond.[29,30] This is also true for γ_x^2, $70\,\mathrm{cm}^{-1}$, as noted above.

In the low-wavenumber infrared spectrum two bands were observed at 195 and ca. $110\,\mathrm{cm}^{-1}$.[12] The higher band is assigned to the rotational mode about the a axis with the lowest moment of inertia.[12,16] On the other hand, the lower band may be assigned to the rotational modes about the other axes and also to the translational modes.[22] The band widths calculated here are 43 and $50\,\mathrm{cm}^{-1}$ for the translational modes and

$63\,cm^{-1}$ for the rotational mode. Since the band width of the lower band is ca. $90\,cm^{-1}$, the band may consist of some components described above.

The damped oscillator model describes vibrational relaxation. Hence, it is not appropriate to apply the present model to a system where rotational relaxation is important. Ojha et al.[23] have reported the isotropic Raman spectrum of $HCONH_2$, where no rotational relaxation is effective. The band widths for ν_4, ν_5, ν_6, and ν_7 were determined to be 20, 62, 15, and $50\,cm^{-1}$, respectively. These values are considerably smaller than those in Table 3, especially in ν_4, suggesting the importance of rotational relaxation in the infrared bands. However, the difference in the band widths between the isotropic Raman and infrared bands is mainly due to intermolecular interactions, giving rise to the non-coincidence effect, which means the difference in the peak positions between the isotropic and anisotropic Raman bands. According to the vibrational coupling model applied to the C=O stretching bands of acetone,[6] the band widths of the isotropic Raman and infrared bands are given as $\Gamma + f^i$ and $\Gamma - f^i$, respectively, where Γ and f^i are the damping constant of two unperturbed oscillators and the damping coupling constant between them, respectively; Γ and f^i of ν_4 are evaluated to be 37 and $-17\,cm^{-1}$, respectively. Since the damping coupling process is vibrational relaxation, the band widths in both the isotropic Raman and infrared bands result from vibrational relaxation in the present system. The difference in the band widths of ν_5–ν_7 is also explained as above. Hence, it is certain that the present analysis on the basis of the vibrational relaxation is reasonable.

As seen above, the band widths in the isotropic Raman and infrared bands differ considerably, especially in the strongly coupled modes. Hence, it is not expected that further information about the damping constants would be obtained from an application of the damped oscillator model to such a spectrum as isotropic Raman.

In the damped oscillator model describing normal modes[1,2] the damping constant is used without clarifying its origin. On the other hand, in the presented study the damping constant is used with a clear physical meaning as a friction constant, by also inferring that c in Eq. 11 should be the velocity in the high frequency mode, i.e., $\dot{\mathbf{X}}$ in Eq. 2, for the velocity of sound in the low frequency mode.[31] Although Eq. 11 could not be applied to the present system as is, it is clear that the damping constant relates to effective force constants on inter- and intramolecular interactions.

Summary

A damped oscillator model has been formulated to analyze entirely the infrared spectrum and has been applied to the in-plane modes of formamide. The main purpose of this study was to clarify how band widths of whole vibrational modes are determined and whether the relation in band widths among whole vibrational modes exists or not. The fact that the infrared spectrum is described reasonably by the damped oscillator model clarifies the origin of the band widths, that is $\Gamma_i = \sum_s \gamma^s l_{si}^2$. The relations of $\gamma_y^2 < \gamma_y^1$ and $\gamma_y^2 < \gamma_x^4$ or γ_y^4 are unexpected from the theory that damping constants result from inter-molecular interactions,[29,30] because the largest interaction is the hydrogen bond in the present system. These suggest the importance of van der Waals forces and the intra-molecular interactions.

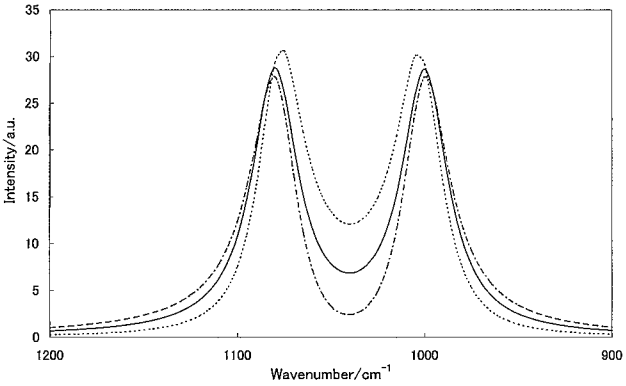

Fig. 3. The infrared spectral changes due to damping coupling. The numerical conditions are: $\nu_m = 1080$, $\nu_n = 1000$, $\Gamma_m = \Gamma_n = 30$, $f^i = -20$ (dashed-dotted line), 0 (solid line) or 20 (dotted line) in cm^{-1} and $T_m = T_n$.

Appendix

As discussed above, the band profile of the i-th mode is given by Eq. 8 with the equality sign, if the off-diagonal terms of Γ^c are zero. We consider two modes given by Eq. 8 with the equality sign, ν_m and ν_n. Since these modes couple with each other through the damping coupling, the infrared spectrum is given as[1–6]

$$S(\nu) = \nu \,\mathrm{Im}\, \tilde{\mathbf{T}}\mathbf{G}(\nu)\mathbf{T}, \tag{A-1}$$

where $\mathbf{G}(\nu)$ and $\tilde{\mathbf{T}}$ are given, respectively, as

$$\mathbf{G}(\nu) = \begin{vmatrix} {\nu_m}^2 - \nu^2 - i\nu\Gamma_m & i\nu f^i \\ i\nu f^i & {\nu_n}^2 - \nu^2 - i\nu\Gamma_n \end{vmatrix}^{-1} \tag{A-2}$$

and

$$\tilde{\mathbf{T}} = \begin{vmatrix} T_m & T_n \end{vmatrix}, \tag{A-3}$$

where f^i is the damping coupling constant and T the intensity parameter. Some results are given in Fig. 3, where the numerical conditions are: $\nu_m = 1080$, $\nu_n = 1000$, $\Gamma_m = \Gamma_n = 30$, $f^i = -20$, 0, or 20 in cm^{-1} and $T_m = T_n$.

In Fig. 3, the infrared spectral features change in the intermediate of two modes, decreasing or increasing in intensity in response to $f^i < 0$ or $f^i > 0$, respectively, as compared with the infrared spectrum with $f^i = 0$, simultaneously increasing or decreasing in intensity in $\nu > \nu_m$ and $\nu < \nu_n$. In these spectra the total intensity is constant independent of f^i. These clearly show that the band profile of the component bands changes from Eq. 8 with the equality sign to a band with large asymmetry. The band profile in the case of $\nu_m = \nu_n$ is discussed in Ref. 6.

Figure 4 shows the band profile of ν_4 and ν_5, whose band constants are given in Table 3. The value of f^i is $-11\,cm^{-1}$. The band profile changes in the intermediate of ν_4 and ν_5, depending on $f^i = 0$ or $-11\,cm^{-1}$, giving rise to a good fit with the observed spectrum given in Fig. 1. This means that the damping constants in Table 2 are adjusted so as to give the off-diagonal element of ν_4 and ν_5 of $-11\,cm^{-1}$, adding the limitation to their values, which may make their reliability high, as noted in the text. Further damping couplings take place among ν_1–ν_9, resulting in high reliability of the damping constants and in the calculated spectrum in Fig. 1; it should be noted that the effect of the damping

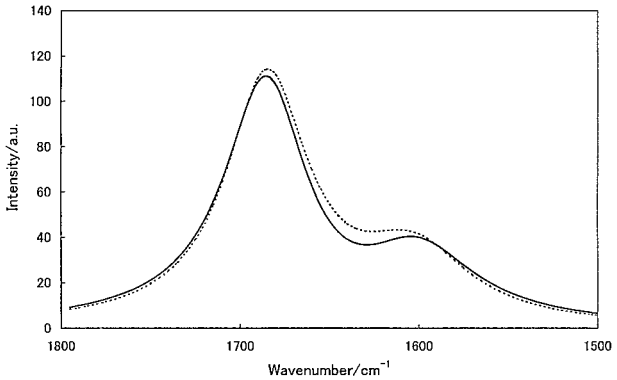

Fig. 4. The band profile on ν_4 and ν_5 by use of the band constants given in Table 3 with $f^i = 0$ (dotted line) or $f^i = -11\,\mathrm{cm}^{-1}$ (solid line).

coupling on the band profile depends, of course, on the separation of ν_m and ν_n.

References

1 A. S. Barker, Jr., J. J. Hopfield, *Phys. Rev.* **1964**, *135*, A1732.
2 A. Chaves, R. S. Katiyar, S. P. S. Porto, *Phys. Rev. B* **1974**, *10*, 3522.
3 I. Kanesaka, *Asian J. Spectrosc.* **2001**, *2*, 57.
4 I. Kanesaka, K. Kobayashi, *J. Mol. Struct.* **2005**, *735–736*, 343.
5 I. Kanesaka, K. Kobayashi, *J. Mol. Struct.* **2005**, *753*, 80.
6 K. Kobayashi, I. Kanesaka, *J. Raman Spectrosc.* **2007**, *38*, 436.
7 G. R. Leader, *J. Am. Chem. Soc.* **1951**, *73*, 856.
8 J. C. Evans, *J. Chem. Phys.* **1954**, *22*, 1228.
9 P. G. Puranik, K. V. Ramiah, *J. Mol. Spectrosc.* **1959**, *3*, 486.
10 I. Suzuki, *Bull. Chem. Soc. Jpn.* **1960**, *33*, 1359.
11 S. T. King, *J. Phys. Chem.* **1971**, *75*, 405.
12 K. Itoh, T. Shimanouchi, *J. Mol. Spectrosc.* **1972**, *42*, 86.
13 C. H. Smith, R. H. Thompson, *J. Mol. Spectrosc.* **1972**, *42*, 227.
14 J. Bukowska, *Spectrochim. Acta, Part A* **1979**, *35*, 985.
15 D. J. Gardiner, A. J. Lees, B. P. Straughan, *J. Mol. Struct.* **1979**, *53*, 15.
16 O. F. Nielsen, P.-A. Lund, E. Praestgaard, *J. Chem. Phys.* **1982**, *77*, 3878.
17 H. Shimizu, K. Nagata, S. Sakaki, *J. Chem. Phys.* **1988**, *89*, 2743.
18 A. Mortensen, O. F. Nielsen, J. Yarwood, V. Shelley, *J. Phys. Chem.* **1994**, *98*, 5221.
19 A. Mortensen, O. F. Nielsen, J. Yarwood, V. Shelley, *J. Phys. Chem.* **1995**, *99*, 4435.
20 A. Mortensen, O. F. Nielsen, J. Yarwood, V. Shelley, *J. Raman Spectrosc.* **1995**, *26*, 669.
21 O. F. Nielsen, A. Mortensen, J. Yarwood, V. Shelley, *J. Mol. Struct.* **1996**, *378*, 1.
22 H. Torii, M. Tasumi, *J. Phys. Chem. B* **1998**, *102*, 315.
23 A. K. Ojha, S. K. Srivastava, J. Koster, M. K. Shukla, J. Leszczynski, B. P. Asthana, W. Kiefer, *J. Mol. Struct.* **2004**, *689*, 127.
24 W. A. Alves, O. A. C. Antunes, E. Hollauer, *Vib. Specrosc.* **2006**, *40*, 257.
25 E. B. Wilson, Jr., J. C. Decius, P. C. Cross, *Molecular Vibrations*, McGraw-Hill, New York, **1955**.
26 R. J. Kurland, E. B. Wilson, Jr., *J. Chem. Phys.* **1957**, *27*, 585.
27 C. C. Costain, J. M. Dowling, *J. Chem. Phys.* **1960**, *32*, 158.
28 E. Hirota, R. Sugisaki, C. J. Nielsen, G. O. Sorensen, *J. Mol. Spectrosc.* **1974**, *49*, 251.
29 P. A. Egelstaff, *An Introduction to the Liquid State*, Academic Press, London, **1967**.
30 S. A. Rice, *Mol. Phys.* **1961**, *4*, 305.
31 S. A. Rice, P. Gray, *The Statistical Mechanics of Simple Liquids*, Wiley, New York, **1965**.